2017 14th International Conference on Ubiquitous Robots and Ambient Intelligence (URAI)
June 28 - July 1, 2017 at Maison Glad Jeju, Jeju, Korea

Differential hysteresis modeling with adaptive parameter estimation of a super-coiled polymer actuator

Tuan Anh Luong[1], Sungwon Seo[1], Ja Choon Koo [1], Hyouk Ryeol Choi[1], Hyungpil Moon [1]
[1]Department of Mechanical Engineering, Sungkyunkwan University, Suwon, 16419, Korea
(Tel : +82-31-290-4842; E-mail: hyungpil@me.skku.ac.kr)

***Abstract*—The super-coiled polymer (SCP) actuator, made from silver coated fishing line which can be actuated by an electric current, is a recently discovered artificial muscle with interesting properties such as large contraction ($20\% - 50\%$), high power density (5.3 kW/kg), light weight and extremely low cost. In this paper, a differential hysteresis model with adaptive parameter estimation is presented for modeling of super-coiled polymer actuators. The operation of the actuator will be modeled with a heat transfer model and strain-temperature hysteresis model. At the heat of the strain-temperature hysteresis modeling is a differential hysteresis model which also incorporates the relationship between hysteresis curves and loads. In addition, adaptive model parameter estimation based on output feedback is applied to increase the performance of the model. The implementation results of the model show that the proposed model can effectively estimate the actuator's behavior, especially its hysteresis. This model can be used to develop a position controller for the super-coiled actuator.**

***Keywords*—Super-coiled polymer actuator, hysteresis modeling, Duhem model, adaptive estimation.**

1. INTRODUCTION

Recently, the introduction of a new class of actuators by Haines [1] has drawn attention of many researchers, due to their interesting properties. The "super-coiled" polymer actuators, made from low-cost materials, were shown to provide large stroke ($20\% - 50\%$), high load-carrying capabilities and especially a high work density of 5.3 kW/kg which exceeds that peak of mammalian skeletal muscles of 0.32 kW/kg [1], [2], [3], [4]. Moreover, Joule heating, a convenient method of controlling actuation, can be implemented by controlling the current through the conductive coating on the surface of the filament. These advantages make conductive SCP actuators good candidates for a future artificial muscle.

Nevertheless, the major challenge in utilizing SCP actuators to achieve accurate perfomance comes from its nonlinearity attributed to hysteresis, creep, etc [4], [5]. In which, especially, as other types of actuators, such as shape memory alloys (SMAs) [6] or McKibben pneumatic actuators [7], hysteresis, which can be as high as 33% [5], might be a serious problem causing degradation of the control performance of SCP actuators. Therefore, it is important to overcome the hysteresis in order to suit SCP actuators for controllable robotic applications.

The successful compensation for hysteresis might rely on the hysteresis modeling. As a good hysteresis model can be utilized in an inverse model to efficiently realize feedforward control or combined with feedback control for precision motion tracking. Since Haines's work, some efforts have been made in order to model the SCP actuators [2], [8], [9], [10]. However, the existing methods are either too complicated to utilize in control as the physics-based model in [9], or simplified linearly [2], [10] that is far from SCP's nonlinear behaviors. Three different models, namely augmented generalized Prandtl-Ishlinskii (GPI), the augmented Preisach model and the augmented linear model were proposed to characterize hysteresis behaviors between voltage input and contraction length of an SCP actuator under different loads in [11]. It is shown that the GPI model was able to capture the hysteresis behavior of SCP actuator with the best performance. However, computation of the weighting function for every point in the hysteresis region is a time-consuming and tedious process. From the control systems point of view, it is advantageous to model the hysteresis using a differential model. Then, the hysteresis can easily be incorporated into the SMA dynamics state space equations. A differential hysteresis model also facilitates the stability analysis of the system. Yet, there is a lack of differential models of SCP hysteresis in the literature.

In this paper, we present our approach for modeling the hysteresis behavior of SCP actuators. The operation of the actuator will be modeled using a heat transfer model and strain-temperature hysteresis model. At the heat of the strain-temperature hysteresis modeling is a differential hysteresis model which also incorporates the relationship between hysteresis curves and loads. Especially, the model's parameters are designed to be adaptively estimated based on output feedback. The effectiveness of our model is verified through simulation and experiments.

The remainder of this paper is organized as follows. Section 2 describes the experimental setup for characterization of the SCP actuator and its properties. The heat-transfer model and temperature control of the actuator are presented in Section 3. Hysteresis modeling are presented in Section 4. Section 5 gives the modeling results and discussions and Section 6 concludes the paper.

978-1-5090-3056-9/17/$31.00 ©2017 IEEE

Authorized licensed use limited to: Universita degli Studi di Bologna. Downloaded on March 22,2022 at 07:58:24 UTC from IEEE Xplore. Restrictions apply.

2. EXPERIMENTAL SETUP FOR ACTUATOR PROPERTY CHARACTERIZATION

2.1. Conductive SCP Actuator

Our methods used to make conductive SCP actuators and for heat treatment are similar to what described in [2]. The material of the actuator is Nylon 6.6 conductive sewing thread (No. 260151023534 from ShieldexTM). In this work, two-ply actuators are used. A weight of $700g$ is used in heat treatment process of the actuator. The lengths of the initial and the finally fabricated (after heat treatment) actuator at the ambient temperature of $T_{amb} = 25°C$ are $110mm$ and $119mm$, respectively. The fabricated actuator is shown in Fig.1.

2.2. Testbed setup

To characterize the SCP actuator, testbeds are developed as shown in Figs. 2a and 2b. Isothermal and isometric tests are carried out using the experimental setup in Fig. 2a, in which one end of the actuator is attached to the testbed, while the opposite end is attached to a load cell (CB1A, 2kgf, DACEL CO.). The distance between the load cell and the testbed can be controlled by a stepper motor (ZCV620-C-N) and a motor controller (DS102, SURUGA SEIKI CO.) with the resolution of $1\mu m$. Electrical leads at the two ends provide the voltage potential across the actuator. For the temperature measurement, a precise thermistor is used. The temperature and the force values are recorded using NI cRIO 9024 and Labview. The thermistor is glued onto the actuator surface using grease (CT250, COOLERTEC).

The experimental setup in Fig. 2b is used to measure the relationship between the actuator's displacement and temperature under different loads. In this experiment, displacement of the SCP actuator will be calculated through an encoder while its temperature is changed. The experiment is repeated for different loads from $200g$ to $600g$. The temperature control for this experiment will be discussed in section 3. The characterization results are shown in Figs. 3 and 4a, 4b. The displacement range and offset of the actuator corresponding to different loads are shown in Figs. 5a and 5b.

It can be concluded that there are severe hysteresis relationships between forces and displacement, and between temperature and displacement, while the hysteresis effect between temperature and force is smaller. The characterization results for the first experimental setup, a model for characterizing force-strain relationship under different temperatures and an control algorithm for SCP actuators have been presented in [12]. In this work, we present our approach for modeling the hysteresis behavior between temperature and displacement under various loads.

3. THERMO-ELECTRIC MODEL AND TEMPERATURE CONTROL OF THE ACTUATOR

In this section, firstly a thermo-electric model (Joule heating model) which represents the relationship between the input power and the temperature state of the actuator is presented.

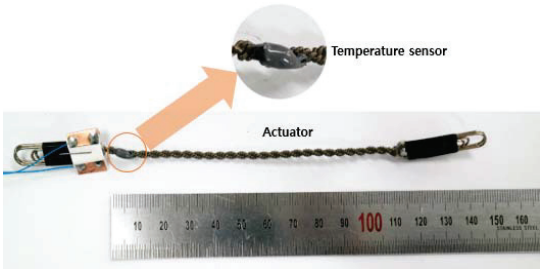

Fig. 1. An SCP actuator fabricated in-house

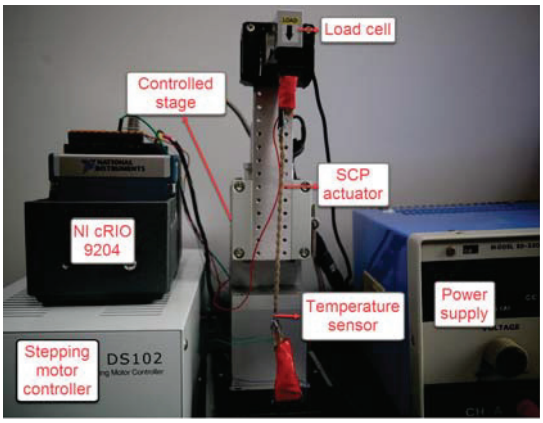

(a) First experimental setup for characterizing the actuator

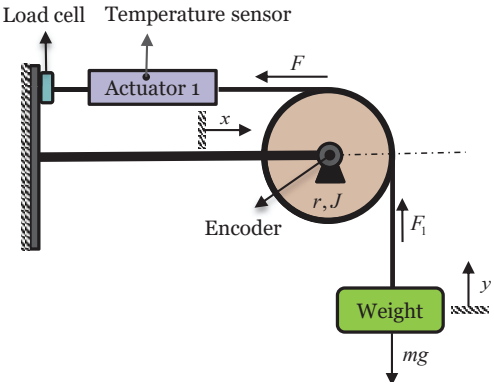

(b) Second experimental setup for characterizating the actuator

Fig. 2. Experimental setup for characterizing the actuator

Based on the model, temperature control of the actuator will be mentioned.

The surface of the SCP actuator is coated with silver wire paste and heated by Joule effect from the external electrical power input. The resistance across the length of the SCP actuator is measured to be $R = 2.5\Omega$ and considered to be constant during the experiment.

A simple thermo-electric model for an SCP actuator is given

Authorized licensed use limited to: Universita degli Studi di Bologna. Downloaded on March 22,2022 at 07:58:24 UTC from IEEE Xplore. Restrictions apply.

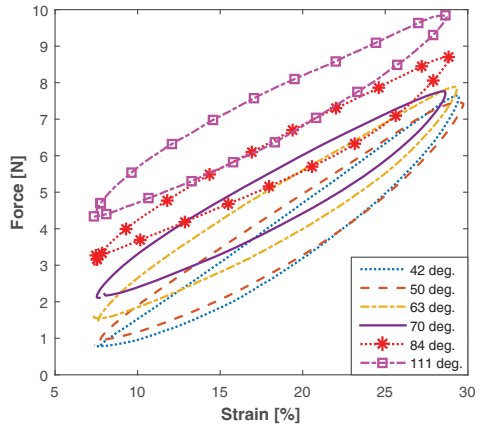

Fig. 3. A force-strain profile of SCP actuators at various temperatures

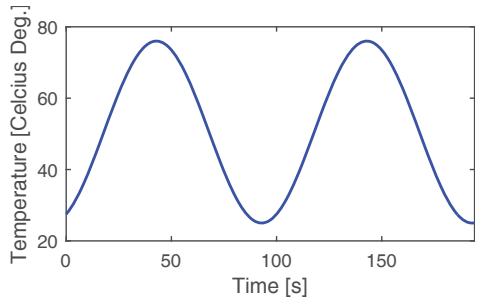

(a) Input temperature

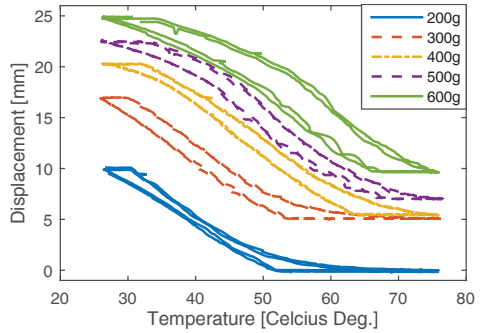

(b) Displacement-Temperature hysteresis under different loads

Fig. 4. Input temperature and the actuator's displacement-temperature hysteresis profiles under different loads

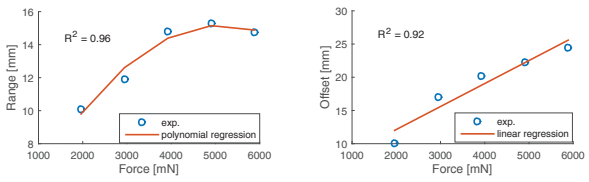

(a) Displacement range (b) Offset

Fig. 5. Diplacement range and offset of the actuator under different loads

as follows [2]:

$$C_{th}\frac{dT(t)}{dt} = P(t) - \lambda(T - T_{amb}) \quad (1)$$

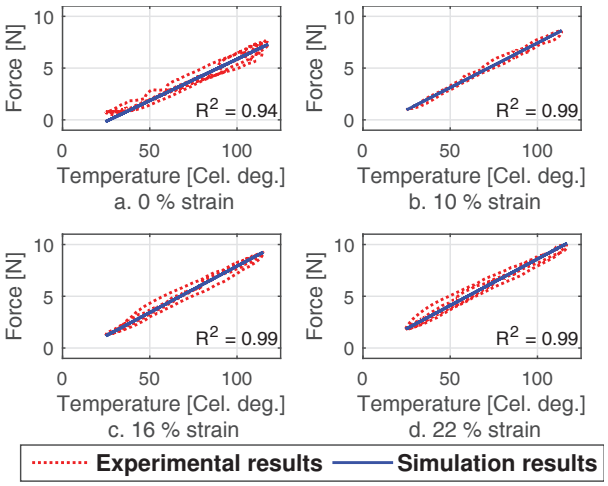

Fig. 6. Temperature-force relationships for various strain conditions

where C_{th} is the thermal mass of the actuator, $P(t) = \frac{V^2}{R}$ is the Joule heating that is applied to the actuator, and λ is the absolute thermal conductivity of the actuator in its ambient environment. The method to find C_{th} and λ can be found in [2]. To increase the cooling speed, in this work, an electric fan (4710KL-05W-B50, Minebea Co. Ltd.) is used. The parameters obtained from the experimental data are shown in Table 1.

TABLE 1
SCP SYSTEM PARAMETERS

Parameter	Value
Actuator's mass m	5 (g)
Resistance R	2.5 (Ω)
a_0	0 (N)
Thermal mass C_{th}	3.92 $(J/^\circ C)$
Heat conductivity λ	0.35 ($W/^\circ C$)
Pulley radius r	0.014 (m)

Based on the model presented in Eq. (1), the temperature of the actuator can be controlled through the power supplied. An adaptive PID sliding mode control (SMC) has been proposed in our previous work [13]. The temperature control performance is illustrated in Fig. 7. It is shown that the temperature can be controlled precisely using our control algorithm.

4. Differential Hysteresis Modeling

In this section, a differential hysteresis model is presented for SCP actuators. The model characterizes the hysteresis behavior between displacement and temperature under different loads. The coefficients of the model are designed to be adaptively updated based on the output feedback.

4.1. Duhem differential model

The Duhem differential model [14] is a phenomenological approach to model hysteresis behavior between an input $u(t)$

Authorized licensed use limited to: Universita degli Studi di Bologna. Downloaded on March 22,2022 at 07:58:24 UTC from IEEE Xplore. Restrictions apply.

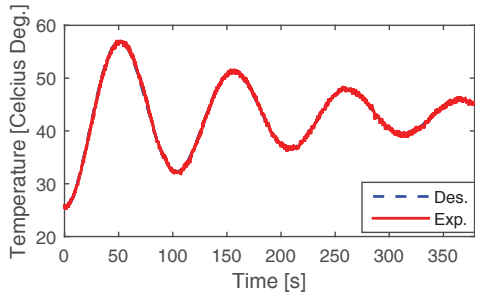

Fig. 7. Temperature control result with a damped waveform

and an output $v(t)$. It is followed intuitively from the fact that if $u(t)$ is an increasing function, then $v(t)$ increases along on a path with the slope g_+, and if $u(t)$ is a decreasing function, then $v(t)$ decreases along another path with the slope g_-. The Duhem model is described as[14]

$$\begin{cases} \dot{v} = g_+(u(t), v(t))(\dot{u})^+ - g_-(u(t), v(t))(\dot{u})^- \\ v(0) = v_0 \end{cases} \tag{2}$$

where $(\dot{u})^{\pm} = \frac{|\dot{u}| \pm (\dot{u})}{2}$ and g_+, g_- are slope functions. Gaussian probability distribution functions (PDFs) was proposed as the slope functions of the major hysteresis loop in [15] as follows

$$g_{+/-}(u) = \frac{1}{\sigma_{+/-}\sqrt{2\pi}} exp(-\frac{(u - \nu_{+/-})^2}{2\sigma_{+/-}^2}) \tag{3}$$

The output v representing the major loop is then given by

$$\begin{aligned} v_{+/-} = h_{+/-}(u) &= \int_{-\infty}^{u} g_{+/-}(u')du' \\ &= \frac{1}{2}\Big[1 + erf(\frac{u - \nu_{+/-}}{\sigma_+\sqrt{2}})\Big] \end{aligned} \tag{4}$$

The major hysteresis loop is given by the differential equation

$$\frac{dv}{du} = \begin{cases} \frac{1}{\sigma_+\sqrt{2\pi}} exp(-\frac{(u-\nu_+)^2}{2\sigma_+^2}), & \dot{u} \geq 0, \\ \frac{1}{\sigma_-\sqrt{2\pi}} exp(-\frac{(u-\nu_-)^2}{2\sigma_-^2}), & \dot{u} < 0. \end{cases} \tag{5}$$

In case of SCP actuators, because it only contracts, it is modified to use $w = 1 - v$ to describe its displacement-temperature hysteresis. To take into account applying loads to the range and offset of the hysteresis curve, from Figs. 5a, 5b, the following model is used

$$x = f_1(F)w(T) + f_2(F) \tag{6}$$

where

$$f_1(F) = a_2F^2 + a_1F + a_0 \tag{7}$$

$$f_2(F) = b_1F + b_0 \tag{8}$$

The model parameters can be identified through an error least squared method. The identification results for a $200g$ load are shown in Fig. 8a and 8b.

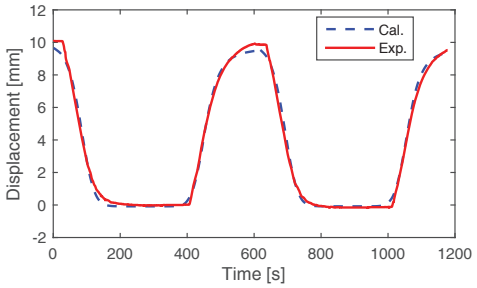

(a) Displacement of the load

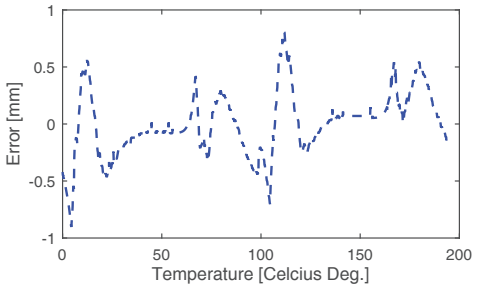

(b) Modeling errors

Fig. 8. Identification results for the 200g load

4.2. Adaptive parameter estimation

During working time, as the model parameters are constant, varying stresses might cause large model errors. One solution for this problem is to employ an adaptive law to update the coefficients a_i $(i = 0..2)$ and b_i $(i = 0, 1)$. The gradient algorithm [16] is used as follows

$$\hat{\boldsymbol{\theta}}^{(i+1)} = \hat{\boldsymbol{\theta}}^{(i)} - \gamma \frac{(\hat{x}^{(i)} - x(i))\boldsymbol{g}(i)}{\boldsymbol{g}(i)^T\boldsymbol{g}(i)}, \tag{9}$$

where $\boldsymbol{\theta} = [a_2, a_1, a_0, b_1, b_0]^T$, $\boldsymbol{g} = [F^2\omega, F\omega, \omega, F, 1]^T$. $\hat{\boldsymbol{\theta}}$ represents the estimated value of $\boldsymbol{\theta}$. By defining

$$\tilde{\boldsymbol{\theta}}^{(i)} = \hat{\boldsymbol{\theta}}^{(i)} - \boldsymbol{\theta}^{(i)} \tag{10}$$

one has

$$\tilde{\boldsymbol{\theta}}^{(i+1)} = \boldsymbol{h}(i)\tilde{\boldsymbol{\theta}}^{(i)} \tag{11}$$

where

$$\boldsymbol{h}^{(i)} = \boldsymbol{I}_5 - \frac{\boldsymbol{g}^{(i)}\boldsymbol{g}^{(i)^T}}{\boldsymbol{g}^{(i)^T}\boldsymbol{g}^{(i)}} \tag{12}$$

where $\boldsymbol{I}_5$ represents the 5×5 identity matrix.

Proposition 1. *The sequence $\boldsymbol{g}^{(i)}$ is persistently exciting if, there exists an integer $N > 0$ and $\beta_1 > 0, \beta_2 > 0$, such that for any n_0*

$$\beta_1\boldsymbol{I}_5 \leq \sum_{n=n_0}^{n_0+N-1} \frac{\boldsymbol{g}(i)\boldsymbol{g}(i)^T}{\boldsymbol{g}(i)^T\boldsymbol{g}(i)} \leq \beta_2\boldsymbol{I}_5 \tag{13}$$

Authorized licensed use limited to: Universita degli Studi di Bologna. Downloaded on March 22,2022 at 07:58:24 UTC from IEEE Xplore. Restrictions apply.

Proposition 2. *If $\boldsymbol{g}^{(i)}$ is persistently exciting, there exists $c_1 > 0$ such that*

$$\left\|\tilde{\boldsymbol{\theta}}^{(i+N)}\right\| \leq \sqrt{1-c_1}\left\|\tilde{\boldsymbol{\theta}}^{(i)}\right\| \tag{14}$$

which guarantees that $\hat{\boldsymbol{\theta}}$ is exponentially convergent.

The proofs for the propositions 1 and 2 can be found in [16]. The condition for the proposition 1 to be satisfied is easily seen due to the bounded property of both function ω and F.

5. Modeling Results and Discussions

After the parameters are identified in Section. 4.1, the displacements of the actuator under other different loads are tested and compared with the model with adaptive parameter estimation algorithm as shown in Figs. 9a-9d. The results show good performance of our proposed model. To test the modeling capability for minor loop of the hysteresis, the damped waveform temperature profile as in Fig. 7 was used. The modeling results shown in Fig. 5 confirm the effectiveness of our model.

For control purpose, the inversion of the model (6) can be expressed as

$$\hat{T} = w^{-1}\left(\frac{x_d - f_2(F)}{f_1(F)}\right) \tag{15}$$

where the Duhem inverse model is

$$\frac{du}{dv} = \begin{cases} \frac{1}{g_+(u)+\delta}, & \dot{u} \geq 0, \\ \frac{1}{g_-(u)+\delta}, & \dot{u} < 0. \end{cases} \tag{16}$$

where $\delta > 0$ is an arbitrarily small constant brought in to prevent the cases when $g_+(u) = 0$ or $g_-(u) = 0$ [15]. From Eq. (1), the required power can be calculated as

$$P(t) = C_{th}\frac{dT(t)}{dt} + \lambda(T - T_{amb}) \tag{17}$$

Eq. (17) can be used as an inversion compensation for controlling the SCP actuator. However, in addition to nonlinear properties of the actuator, it is noted that the temperature which is measured using a thermistor at only one small region of the actuator might be not the same along the actuator's length. Those might make the inversion compensation model insufficient for controlling the displacement of the actuator. Therefore, it is necessary to combine the inversion compensation with a feedback control law to improve the tracking results of the actuator. An example of such combination can be seen in the diagram shown in Fig. 5.

6. CONCLUSIONS

In this paper, a differential hysteresis model with output based adaptive parameter estimation was presented. The model was shown to successfully capture the hysteresis behavior of the actuators. The advantage of this model is that it can easily be incorporated into the SCP dynamics state space equations. It can also facilitate the stability analysis of the system.

A major challenge in using SCP actuators is their low speed of operation resulting from the slow heat transfer dynamics.

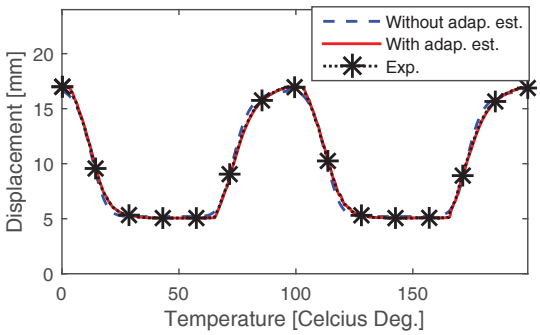

(a) 300g load

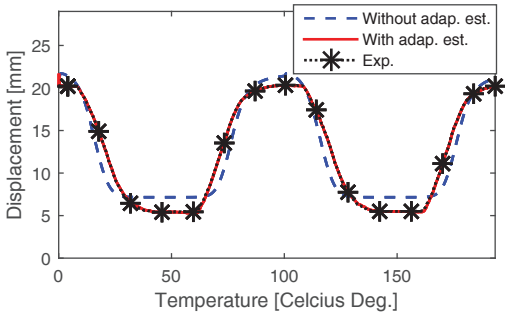

(b) 400g load

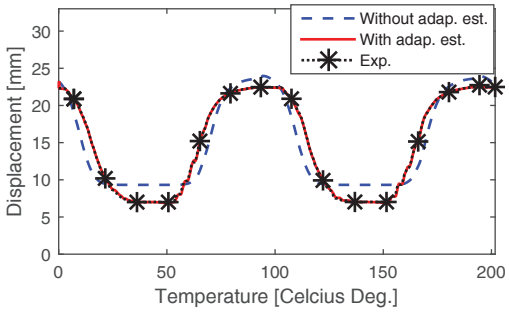

(c) 500g load

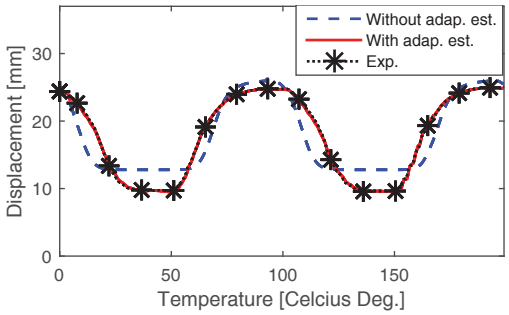

(d) 600g load

Fig. 9. Modeling results under different loads

For better speed of the actuator, the use of methods for improving cooling speed of SCP actuators is necessary. The antagonistic joint, which is actuated by a pair of agonist and antagonist actuator is one of the configuration that has

Authorized licensed use limited to: Universita degli Studi di Bologna. Downloaded on March 22,2022 at 07:58:24 UTC from IEEE Xplore. Restrictions apply.

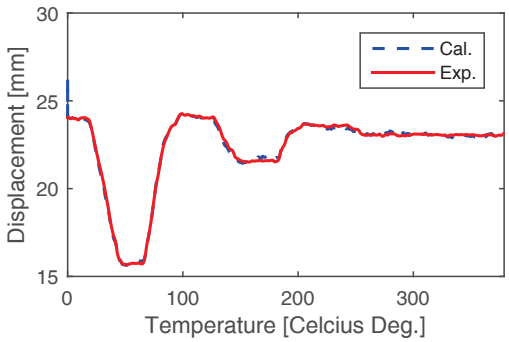

Fig. 10. Modeling results for a damped waveform with the load of 600g

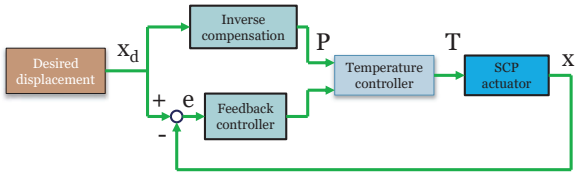

Fig. 11. A control block diagram based on the proposed model

good controllability and response properties. However, in the differential configuration, each SCP actuator is subjected to a time-varying stress, which might induce big errors to the models that consider constant loads only . Our future work will also include research of appling our model with adaptive parameter estimation for the antagonistic joint analysis and control.

ACKNOWLEDGMENT

This research was supported by the convergence technology development program for bionic arm through the National Research Foundation of Korea (NRF) funded by the Ministry of Science, ICT and Future Planning (No. 2014M3C1B2048175).

REFERENCES

[1] C. S. Haines, M. D. Lima, N. Li, G. M. Spinks, J. Foroughi, J. D. Madden, S. H. Kim, S. Fang, M. J. de Andrade, F. Göktepe, *et al.*, "Artificial muscles from fishing line and sewing thread," *science*, vol. 343, no. 6173, pp. 868–872, 2014.

[2] M. C. Yip and G. Niemeyer, "High-performance robotic muscles from conductive nylon sewing thread," in *Robotics and Automation (ICRA), 2015 IEEE International Conference on*, pp. 2313–2318, IEEE, 2015.

[3] S. M. Mirvakili, A. R. Ravandi, I. W. Hunter, C. S. Haines, N. Li, J. Foroughi, S. Naficy, G. M. Spinks, R. H. Baughman, and J. D. Madden, "Simple and strong: Twisted silver painted nylon artificial muscle actuated by joule heating," in *SPIE Smart Structures and Materials+ Nondestructive Evaluation and Health Monitoring*, pp. 90560I–90560I, International Society for Optics and Photonics, 2014.

[4] S. Kianzad, M. Pandit, A. Bahi, A. R. Ravandi, F. Ko, G. M. Spinks, and J. D. Madden, "Nylon coil actuator operating temperature range and stiffness," in *SPIE Smart Structures and Materials+ Nondestructive Evaluation and Health Monitoring*, pp. 94301X–94301X, International Society for Optics and Photonics, 2015.

[5] A. Cherubini, G. Moretti, R. Vertechy, and M. Fontana, "Experimental characterization of thermally-activated artificial muscles based on coiled nylon fishing lines," *AIP Advances*, vol. 5, no. 6, p. 067158, 2015.

[6] A. Pruski and H. Kihl, "Shape memory alloy hysteresis," *Sensors and Actuators A: Physical*, vol. 36, no. 1, pp. 29–35, 1993.

[7] C.-P. Chou and B. Hannaford, "Measurement and modeling of mckibben pneumatic artificial muscles," *Robotics and Automation, IEEE Transactions on*, vol. 12, no. 1, pp. 90–102, 1996.

[8] S. Sharafi and G. Li, "A multiscale approach for modeling actuation response of polymeric artificial muscles," *Soft matter*, vol. 11, no. 19, pp. 3833–3843, 2015.

[9] Q. Yang and G. Li, "A top-down multi-scale modeling for actuation response of polymeric artificial muscles," *Journal of the Mechanics and Physics of Solids*, vol. 92, pp. 237–259, 2016.

[10] T. Arakawa, K. Takagi, K. Tahara, and K. Asaka, "Position control of fishing line artificial muscles (coiled polymer actuators) from nylon thread," in *SPIE Smart Structures and Materials+ Nondestructive Evaluation and Health Monitoring*, pp. 97982W–97982W, International Society for Optics and Photonics, 2016.

[11] J. Zhang, K. Iyer, A. Simeonov, and M. C. Yip, "Modeling and inverse compensation of hysteresis in supercoiled polymer artificial muscles," *IEEE Robotics and Automation Letters*, vol. 2, no. 2, pp. 773–780, 2017.

[12] T. Luong, K. Cho, M. Song, J. Koo, H. R. Choi, and H. Moon, "Nonlinear tracking control of a conductive super-coiled polymer actuator," *Soft Robotics. Under review*.

[13] T. Luong, S. Seo, H. Choi, and H. Moon, "Adaptive pid sliding mode control for motion tracking of super coiled actuators," in *12th Korea Robotics Society Annual Conference (KRoC)*, 2017.

[14] A. Visintin, *Differential models of hysteresis*, vol. 111. Springer Science & Business Media, 2013.

[15] S. M. Dutta and F. H. Ghorbel, "Differential hysteresis modeling of a shape memory alloy wire actuator," *IEEE/ASME Transactions on Mechatronics*, vol. 10, no. 2, pp. 189–197, 2005.

[16] G. C. Goodwin and K. S. Sin, *Adaptive filtering prediction and control*. Courier Corporation, 2014.

Authorized licensed use limited to: Universita degli Studi di Bologna. Downloaded on March 22,2022 at 07:58:24 UTC from IEEE Xplore. Restrictions apply.